UDC 621.313 **doi: 10.20998/2074-272X.2020.4.02**

M. Ben Slimene

PERFORMANCE ANALYSIS OF SIX-PHASE INDUCTION MACHINE-MULTILEVEL INVERTER WITH ARBITRARY DISPLACEMENT

Purpose. This paper presents a d-q model of six-phase induction machine supplied by a two identical voltage source inverters suitable for analysis the dynamic steady under balanced operating condition. In the analytical model, the effects of common mutual leakage inductance between the dual stator have been included. The model has been developed in general reference frame taking into account of 0°, 30° and 60° displacements between two stator winding sets. The main purpose of this work is to conduct a quantitative study to show the advantage of supplying the six-phase induction machine by a multilevel inverter. The voltage and current total harmonic distortion and the torque ripple rate are the main targets. This paper is organized into four sections. After the introduction, the second section includes development of mathematical models concerning the six-phase induction machine. The third presents the effect of displacements of 0°, 30 ° and 60 ° between two stator-winding sets, and a comparison of three cases. After that, we present a comparative study between two, three, five and seven inverter levels when feeding the six-phase induction machine. For this purpose, simulations were carried out to obtain phase currents and torque ripple rates in steady state. References 13, tables 2, figures 13.

Key words: **six phase induction machine, multiphase electric drives, multiphase machines performance, displacements, multi-level inverter.**

Цель. В статье представлена d-q модель шестифазной асинхронной машины, снабженной двумя идентичными инверторами источника напряжения, пригодными для анализа динамической устойчивости при сбалансированных условиях работы. В аналитическую модель включено влияние общей взаимной индуктивности рассеяния между двойным статором. Модель разработана в общей системе отсчета с учетом смещений на 0°, 30° и 60° между двумя наборами обмоток статора. Основная цель данной работы – провести количественное исследование, чтобы показать преимущество питания шестифазной асинхронной машины многоуровневым инвертором. Общее гармоническое искажение напряжения, тока и пульсация крутящего момента являются основными целями исследования. Статья состоит из четырех разделов. После введения, второй раздел содержит разработку математических моделей применительно к шестифазной асинхронной машине. В третьем разделе представлено влияние смещения на 0°, 30° и 60° между двумя наборами обмоток статора, а также сравнение трех указанных случаев. После этого представлено сравнительное исследование двух, трех, пяти и семи уровней инвертора при питании шестифазной асинхронной машины. Для этой цели проведено моделирование с целью получения фазных токов и пульсаций крутящего момента в стационарном состоянии. Библ. 13, табл. 2, рис. 13.

Ключевые слова: **шестифазная асинхронная машина, многофазные электроприводы, производительность многофазных машин, смещения, многоуровневый инвертор.**

Introduction. Multi-phase induction machine has many advantages over conventional three-phase such as reducing torque pulsation, reducing the stator current per phase without increasing the voltage per phase, reducing the rotor harmonic current and higher reliability [1, 2]. In particular, with loss of one or more of stator winding excitation sets, a multi-phase induction machine can continue to be operated with an asymmetrical winding structure and unbalanced excitation, [1].

By dividing the required power between multiple phases, higher power levels can be obtained and the limits of number of machine phases have been removed when employing voltage source inverter [3]. The use of multi-phase machines permits to take advantage of additional degrees of freedom but is likely limited to specialized applications such as electric/hybrid vehicles, aerospace applications, ship propulsion, and high power application [3, 4]. In the literature, a variety of transformations has been proposed for the analysis for multi-phase induction machine.

T.A. Lipo [5] and G.K. Singh [1, 6, 7] derived a *d-q* model for a six-phase machine in dynamic and sinusoidal steady state; the slot leakage coupling between two stators winding sets was incorporated into the model. T.A. Lipo has explained this in detail and has given the technique for finding the slot reactance. Y. Zhao [8] and M.A. Abbas [2] have reported the model for six-phase induction machine supplied by PWM inverter with spatially phase shifted by 30 electrical degrees and where mutual leakage inductances are neglected. R.H. Nelson [9] carried out simulation on three types of six-phase machine using a voltage source inverter where the dual stators are shifted by 0, 30 and 60 electrical degrees and mutual leakage inductances are neglected. Nevertheless, there have been studies where the mutual leakage inductance has been neglected [2, 5, 7-13].

In this paper, an analytical *d-q* model of six-phase induction machine has been developed in a general reference frame and the effect of mutual leakage inductance has been included. The presence of the mutual leakage impedance between the two stars of induction generator is due to the fact their windings share the same slots, and are, therefore, mutually coupled. The mutual leakage coupling has an important effect on the harmonic coupling between the two stator winding sets and depends on the winding pitch and the displacement angle between the two stator winding sets. Subsequently, the six phase induction machine (SPIM) is fed by two identical source inverters taking into account of 0°, 30° and 60° displacements between two stators winding sets and a comparison of three cases has been presented.

The **purpose** of this work is to conduct a quantitative study to show the advantage of supplying the six-phase induction machine by a multilevel inverter.

Modeling of six-phase induction machine. More than three phase windings are housed in the same stator in a multiphase induction motor and thus the current per

phase in the motor is reduced. Two sets of three phase windings are moved by 30° electrical spatially (Fig. 1) in the most typical of these structures.

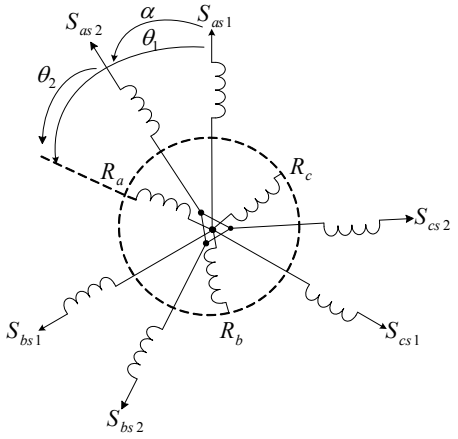

Fig. 1. Schematic representation of the SPIM

In the Fig. 2 the common mutual leakage inductance represents the fact that the two sets of stator windings occupy the same slots mutually coupled by a component of leakage flux.

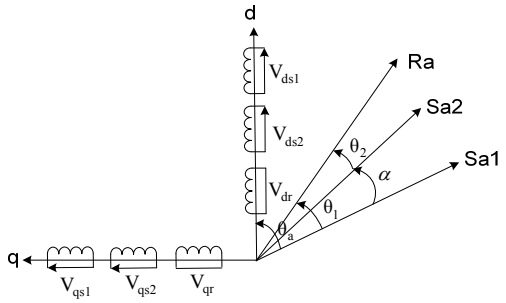

Fig. 2. *d-q* transformation of the SPIM

The electric equations of stator 1, stator 2 and of rotor are respectively expressed by:

$$\left[V_{abc,s1}\right]=\left[R_{s1}\right]\cdot\left[I_{abc,s1}\right]+\frac{d}{dt}\left[\psi_{abc,s1}\right]; \quad (1)$$

$$\left[V_{abc,s2}\right]=\left[R_{s2}\right]\cdot\left[I_{abc,s2}\right]+\frac{d}{dt}\left[\psi_{abc,s2}\right]; \quad (2)$$

$$\left[V_{abc,r}\right]=\left[R_{s1}\right]\cdot\left[I_{abc,r}\right]+\frac{d}{dt}\left[\psi_{abc,r}\right]. \quad (3)$$

The model is based on Park transformation of a three phase system of axes (*a*, *b*, *c*) a two-phase equivalent system of axes (*d*, *q*) creating the same magneto motive force. During the application of the *d-q* transformation and making the necessary manipulations, the equations (1) – (3) in *d-q* become

$$V_{ds1}=R_{s1}i_{ds1}+\frac{d\psi_{ds1}}{dt}-w_a\psi_{qs1}; \quad (4)$$

$$V_{qs1}=R_{s1}i_{qs1}+\frac{d\psi_{qs1}}{dt}+w_a\psi_{ds1}; \quad (5)$$

$$V_{ds2}=R_{s2}i_{ds2}+\frac{d\psi_{ds2}}{dt}-w_a\psi_{qs2}; \quad (6)$$

$$V_{qs2}=R_{s2}i_{qs2}+\frac{d\psi_{qs2}}{dt}+w_a\psi_{ds2}; \quad (7)$$

$$0=R_ri_{dr}+\frac{d\psi_{dr}}{dt}-(w_a-w)\psi_{qr}; \quad (8)$$

$$0=R_ri_{qr}+\frac{d\psi_{qr}}{dt}+(w_a-w)\psi_{dr}, \quad (9)$$

where w is speed of rotation of the coordinate (d, q) relative to the rotor; w_a is speed of rotation of the coordinate (d, q) relative to the stator 1.

Equations of flux are

$$\psi_{ds1}=L_si_{ds1}+L_{ps}i_{ds2}+Mi_{dr}; \quad (10)$$

$$\psi_{qs1}=L_si_{qs1}+L_{ps}i_{qs2}+Mi_{qr}; \quad (11)$$

$$\psi_{ds2}=L_si_{ds2}+L_{ps}i_{ds1}+Mi_{dr}; \quad (12)$$

$$\psi_{qs2}=L_si_{qs2}+L_{ps}i_{qs1}+Mi_{qr}; \quad (13)$$

$$\psi_{dr}=L_ri_{dr}+Mi_{ds1}+Mi_{ds2}; \quad (14)$$

$$\psi_{qr}=L_ri_{qr}+Mi_{qs1}+Mi_{qs2}, \quad (15)$$

where $L_s = L_{s1} = L_{s2} = l_{s1} + l_{sm} + L_m$ – the cyclic inductance of the stator; $L_r = l_r + L_m$ – the cyclic inductance of the rotor; $L_{ps} = l_{sm} + L_m$ – the cyclic mutual inductance between stator 1 and stator 2; L_m – the mutual inductance between stator 1, stator 2 and the rotor; l_{sm} – the mutual leakage inductance between stator 1 and stator 2; l_{s1}, l_{s2} – the stator leakage inductance; l_r – the rotor leakage inductance; R_s – the stator resistance; R_r – the rotor resistance.

The electromagnetic torque can be expressed as

$$C_{em}=n_p\frac{M}{L_r}\left[\left(i_{qs1}+i_{qs2}\right)\psi_{dr}-\left(i_{ds1}+i_{ds2}\right)\psi_{qr}\right]. \quad (16)$$

The analytical *d*-model is developed in a general reference frame and can be used to analyze the behavior of induction machine in any reference frame (Fig. 3).

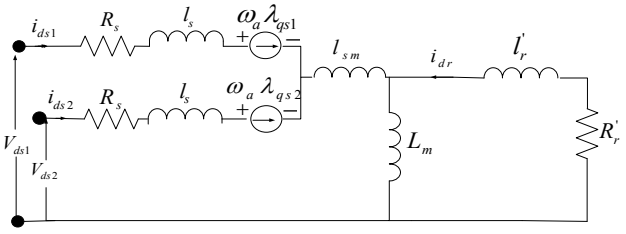

Fig. 3. d-axis equivalent circuit of a SPIM in arbitrary reference frame

The state equation of the form:

$$\dot{X}=AX+BU,$$

where

$X=\left[i_{ds1},i_{qs1},i_{ds2},i_{qs2},\psi_{dr},\psi_{qr}\right]$ – state vector;

$U=\left[V_{ds1},V_{qs1},V_{ds2},V_{qs2}\right]$ – input vector.

After a calculation, we obtain the following matrices

$$A=\begin{bmatrix} -\frac{a_{11}}{a_1} & w_a & -\frac{b_{11}}{a_1} & 0 & \frac{d_1}{a_1T_r} & \frac{d_1}{a_1}w \\ -w_a & -\frac{a_{11}}{a_1} & 0 & -\frac{b_{11}}{a_1} & -\frac{d_1}{a_1}w & \frac{d_1}{a_1T_r} \\ -\frac{b_{11}}{a_1} & 0 & -\frac{a_{11}}{a_1} & w_a & \frac{d_1}{a_1T_r} & \frac{d_1}{a_1}w \\ 0 & -\frac{b_{11}}{a_1} & -w_a & -\frac{a_{11}}{a_1} & -\frac{d_1}{a_1}w & \frac{d_1}{a_1T_r} \\ \frac{M}{T_r} & 0 & \frac{M}{T_r} & 0 & -\frac{1}{T_r} & (w_a-w) \\ 0 & \frac{M}{T_r} & 0 & \frac{M}{T_r} & -(w_a-w) & -\frac{1}{T_r} \end{bmatrix}; \quad (17)$$

$$B=\begin{bmatrix} \frac{1}{a_1} & 0 & -\frac{b_1}{a_1} & 0 \\ 0 & \frac{1}{a_1} & 0 & -\frac{b_1}{a_1} \\ -\frac{b_1}{a_1} & 0 & \frac{1}{a_1} & 0 \\ 0 & -\frac{b_1}{a_1} & 0 & \frac{1}{a_1} \\ 0 & 0 & 0 & 0 \\ 0 & 0 & 0 & 0 \end{bmatrix}, \quad (18)$$

where

$$a_1=\sigma_1 L_s-\frac{(\sigma_2 L_{ps})^2}{\sigma_1 L_s}, \quad b_1=\frac{\sigma_2 L_{ps}}{\sigma_1 L_s}, \quad c_1=\frac{\sigma_2 L_{ps}}{\sigma_1 T_s},$$

$$d_1=\left(1-\frac{\sigma_2 L_{ps}}{\sigma_1 L_s}\right)\frac{M}{L_r}, \quad a_{11}=R_s+\frac{d_1 M}{T_r}, \quad b_{11}=\frac{d_1 M}{T_r}-c_1,$$

$$\sigma_1=1-\frac{M^2}{L_s L_r}, \quad \sigma_2=1-\frac{M^2}{L_{ps} L_r}, \quad T_r=\frac{L_r}{R_r}, \quad T_s=\frac{L_s}{R_S}.$$

Simulation results of the SPIM with arbitrary displacements. In this section, the simulation results for the generalized theory of machine is presented. The dynamic performance behavior of the six-phase machine was determined, and implemented in Matlab/Simulink environment. This simulation results are generated in the Matlab/Simulink environment for the machine performance characteristics. The performance behavior of the machine was determined using the equivalent circuit. To observe the behavior of a six-phase induction machine, the nonlinear mixed model «stator current-rotor flux», which describes the SPIM, was analyzed and simulated. The machine used is characterized by a two poles, 250 V per phase, frequency 50 Hz, and nominal speed 2880 rpm. Figure 4 shows the block diagram necessary to undertake the simulation.

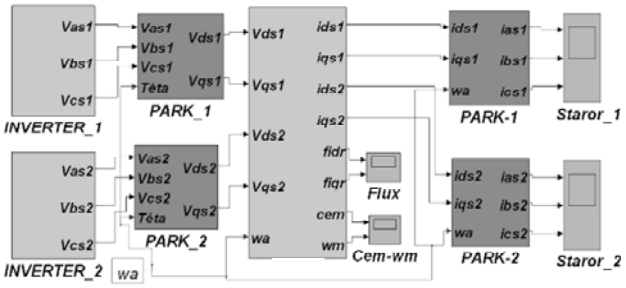

Fig. 4. Simulink structural scheme of six-phase induction machine model

The operating characteristics of the simulation test machine supplied by two identical voltage source inverters are illustrated at Fig. 5, 6 for the displacement angle 0°, 30° and 60° respectively.

The operating is characterized by an unloading start-up and then inserting the load torque from t = 1 s. In the Table 1 presents the torque ripple with different position of angle between the two stator.

Table 1

Torque ripple with displacement angle

Displacement	ΔC_{em}, %
$\alpha = 0°$	9.4
$\alpha = 30°$	3.1
$\alpha = 60°$	9.4

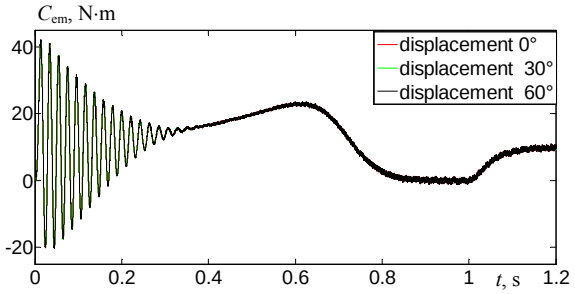

Fig. 5. Characteristic of the electromagnetic torque

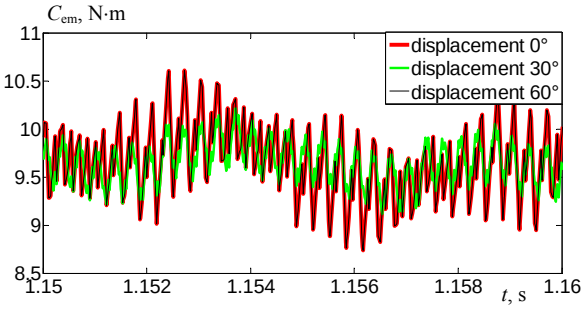

Fig. 6. Zoom on the steady state of electromagnetic torque

Heir it has been clearly shown through results that by varying displacement from low to high value we can minimize the total harmonic distortion (THD) of rotor currents (Fig. 7, 8). The variations in modulation index also affect the speed of six phase induction motor drive. There are fluctuations in the starting of rotor currents and electromagnetic torque.

The performance of a six phase induction motor operating under supply unbalance displacement (0°, 30°, 60°) show in the Fig. 7, 8.

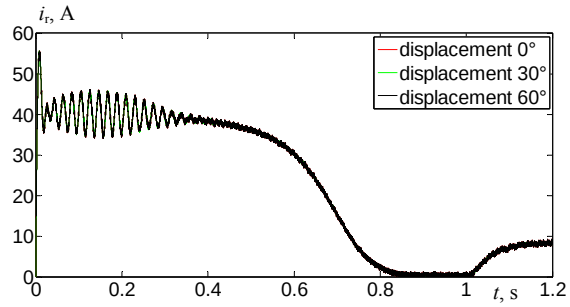

Fig. 7. Characteristic of rotor current i_r

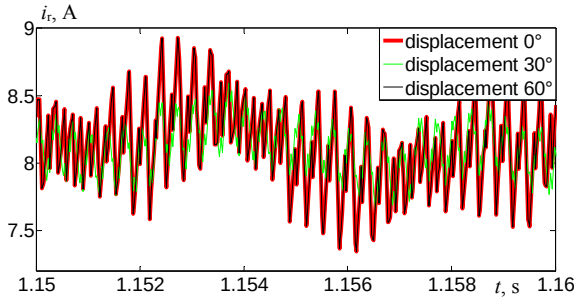

Fig. 8. Zoom on the steady state of rotor current

In Fig. 9, 10 we present the effect of the displacement in the stator current i_{as1}. This results investigates the significance of supply phase shift on the performance of a six induction motor by applying a novel phase shift unbalance definition to the negative and positive sequence components model of the SPIM. The test results reveal that when both phase angle shift and voltage magnitude unbalance occur simultaneously the effect of the phase shift dominates over the effects of the voltage magnitude unbalance. This study shows that phase angle unbalance has a severe consequence on six phase machine performance.

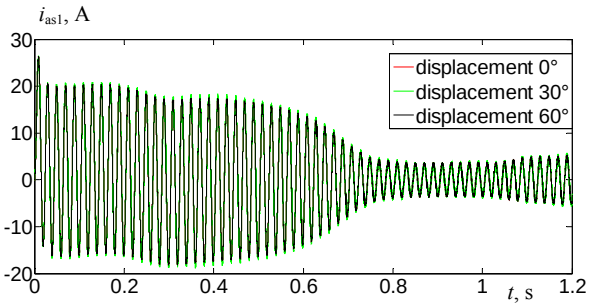

Fig. 9. Characteristic of stator current i_{as1} per phase «A»

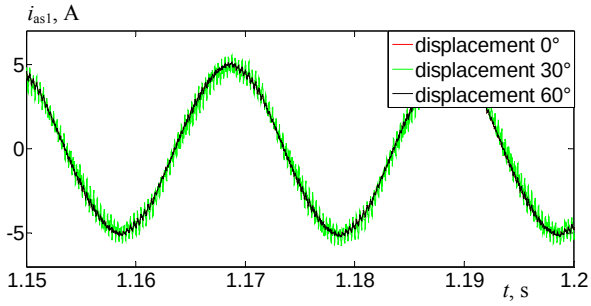

Fig. 10. Appearance of current i_{as1}

Simulation results of the SPIM fed by a multilevel inverter. We aim, in this section, to compare the quality of various wave quantities, namely the line to line voltages, winding currents and electromagnetic torque.

For each m level inverter, the simulation results will include the waves previously mentioned and their THD.

The inverters output voltages or winding voltages are displayed in Fig. 11. The number of levels generated by each inverter can be easily identified from the waveforms. The feeding voltages of the motor, represented in (d, q) axes, are function of the line to line multilevel inverter voltages shown in Fig. 11. These latter will be concerned by the following harmonics study.

During the starting, Fig. 12 shows the electromagnetic torque oscillating in the first moments. The transient torque may reach a peak of 5 N·m. At t = 0.5 s, a load torque of 3 N·m is applied. Besides, the impact of the inverter output voltage quality on the rotor torque is especially visible during the steady state.

In fact, Fig. 12 clearly illustrates that the torque ripple during steady state period decreases gradually and progressively as the inverter number of levels increases. Relative results are resumed in Table 2. It has to be emphasized that less torque ripple leads to better stability operation with minimum mechanical noise.

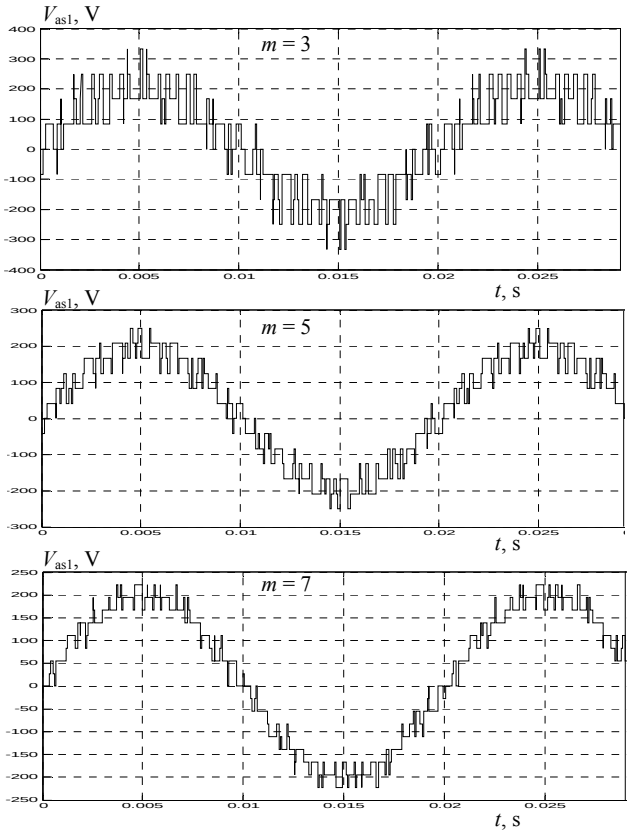

Fig. 11. Waveform of output voltage V_{as1} for m = 3, 5, 7

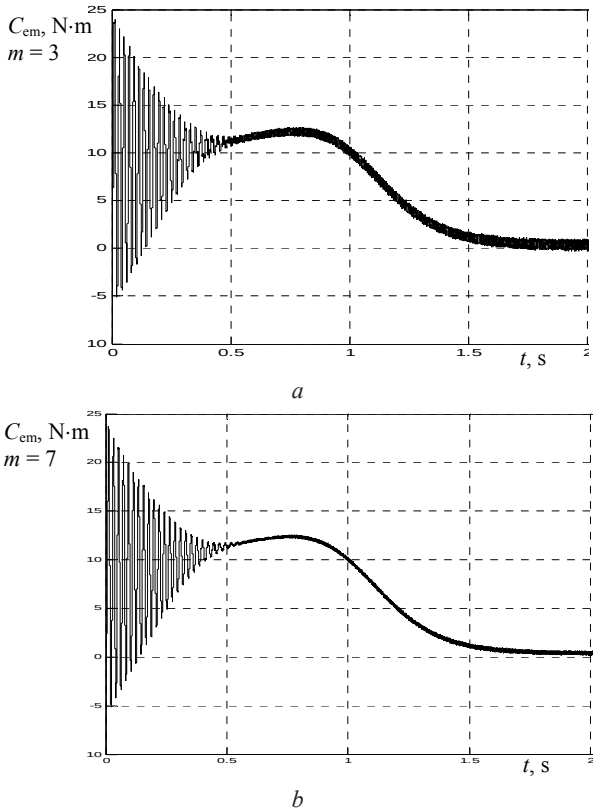

Fig. 12. Electromagnetic torque for m = 3 (a) and m = 7 (b)

In order to compare the quality of electromagnetic torque, Table 2 details ripple rate of 3 and 7 multilevel inverter output voltages. It also displays the THD corresponding to different voltage levels up to m = 7.

Table 2

Torque ripple with inverter levels number

Levels number	Relative torque ripple rate in %
$m = 3$	10.52
$m = 7$	4.96

Figure 13 gives the general shape of the absorbed current during the transient state. In addition, the steady state current, its spectral analysis and its THD are detailed. If the voltage level changes from $m = 3$ to $m = 7$, the THD drops from 4.03 % to 2.12 %. As can be seen, the THD varies slowly upper to 5 levels.

The stepped voltage waveform is composed by m levels, which depends on DC sources numbers, such that $m = 2S + 1$. Thus, whatever is the type of cascaded multilevel inverter, the output voltage levels number is always odd (3, 5, 7, 11, ...).

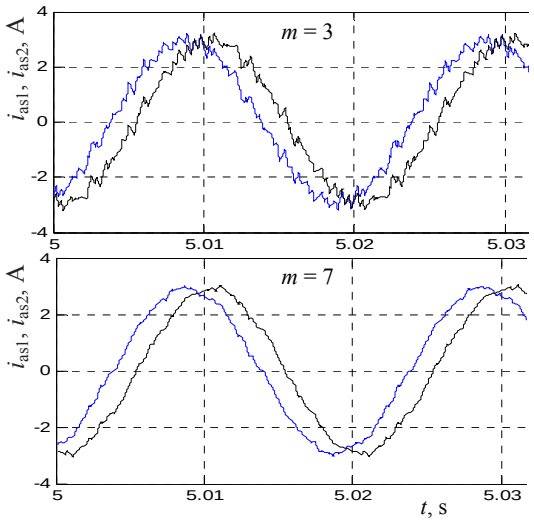

Fig. 13. Stator currents i_{as1}, i_{as2} for $m = 3, 7$ respectively

Conclusion.

This paper demonstrates the stepwise development of six phase induction machine model to simulate the starting and dynamic behaviors of six-phase split winding induction machines fed by multilevel inverter. The free acceleration characteristics as well as the dynamic response with level inverter variation were tested on the simulation and the results were likewise displayed. This paper also, has investigated the operational impact of supply phase shift on the performance of six-phase induction machine. The phase shift unbalance causes a reduction in motor efficiency, developed torque, and motor power factor. It also leads to undesirable increase in reactive power consumption, which increases energy cost. In the next work we will study the impact of the sensitivity of the mutual leakage flux of SPIM fed by multilevel inverter, we will consider three possible cases where first the mutual leakage flux is suitably modelled, second it is considered as a self-leakage flux and finally it is totally ignored.

REFERENCES

1. Singh G.K., Pant V., Singh Y.P. Voltage source inverter driven multi-phase induction machine. *Computers and Electrical Engineering*, 2003, vol. 29, no. 8, pp. 813-834. **doi: 10.1016/s0045-7906(03)00036-3.**

2. Abbas M.A., Christen R., Jahns T.M. Six-Phase Voltage Source Inverter Driven Induction Motor. *IEEE Transactions on Industry Applications*, 1984, vol. IA-20, no. 5, pp. 1251-1259. **doi: 10.1109/tia.1984.4504591**.

3. Gupta N., Singh Y. Stability and response of extremum seeking feedback scheme for squirrel cage induction generator based WECS. *International Journal of Advanced and Applied Sciences*, 2017, vol. 4, no. 6, pp. 50-55. **doi: 10.21833/ijaas.2017.06.007.**

4. Miranda R.S., Jacobina C.B., Lima A.M.N. Modeling and analysis of six-phase induction machine under fault condition. *2009 Brazilian Power Electronics Conference*, 2009, pp. 824-829. **doi: 10.1109/cobep.2009.5347696.**

5. Lipo T.A. A d-q model for six phase induction machine. *International Conference on Electrical Machines ICEM*, Athens, Greece, 1980, pp. 860-867.

6. Singh G.K., Singh D.K.P., Nam K., Lim S.K. A simple indirect field-oriented control scheme for multiconverter-fed induction motor. *IEEE Transactions on Industrial Electronics*, 2005, vol. 52, no. 6, pp. 1653-1659. **doi: 10.1109/tie.2005.858707.**

7. Pant V., Singh G.K., Singh S.N. Modeling of a multi-phase induction machine under fault condition. *Proceedings of the IEEE 1999 International Conference on Power Electronics and Drive Systems. PEDS'99* (Cat. No.99TH8475), 1999. **doi: 10.1109/peds.1999.794542.**

8. Zhao Y., Lipo T.A. Modeling and control of a multi-phase induction machine with structural unbalance. *IEEE Transactions on Energy Conversion*, 1996, vol. 11, no. 3, pp. 570-577. **doi: 10.1109/60.537009.**

9. Nelson R., Krause P. Induction machine analysis for arbitrary displacement between multiple winding sets. *IEEE Transactions on Power Apparatus and Systems*, 1974, vol. PAS-93, no. 3, pp. 841-848. **doi: 10.1109/tpas.1974.293983**.

10. Khlifi M.A. Analysis of an off-grid self-excited dual wound asynchronous generator for wind power generation. *International Journal of Advanced and Applied Sciences*, 2019, vol. 6, no. 6, pp. 35-42. **doi: 10.21833/ijaas.2019.06.006**.

11. Marwa B.S., Larbi K.M., Mouldi B.F., Habib R. Modeling and analysis of double stator induction machine supplied by a multi level inverter. *2012 16th IEEE Mediterranean Electrotechnical Conference*, March 2012, pp. 269-272. **doi: 10.1109/melcon.2012.6196430.**

12. Tuballa M.L., Abundo M.L.S. Microgrid simulation and modeling for a utility in southern Negros Oriental, Philippines. *International Journal of Advanced and Applied Sciences*, 2018, vol. 5, no. 7, pp. 86-96. **doi: 10.21833/ijaas.2018.07.011.**

13. Al Ahmadi S., Khlifi M.A., Draou A. Voltage and frequency regulation for autonomous induction generators in small wind power plant. *International Journal of Advanced and Applied Sciences*, 2019, vol. 6, no. 1, pp. 95-98. **doi: 10.21833/ijaas.2019.01.013.**

Received 22.06.2020

Ben Slimene Marwa, Ph.D, Assistant Professor,
College of Computer Science and Engineering,
University of Hail, Hail, Kingdom of Saudi Arabia,
22, Aljouf Str., Hail, Kingdom of Saudi Arabia, 8080.
e-mail: Benslimene.marwa@gmail.com